Warm Dark Matter Collapse

real space analysis methods

by

Jonathan Loranger

B.Sc., The University of Guelph, 2010

A THESIS SUBMITTED IN PARTIAL FULFILLMENT OF
THE REQUIREMENTS FOR THE DEGREE OF

MASTER OF SCIENCE

in

The Faculty of Graduate and Postdoctoral Studies

(Physics)

THE UNIVERSITY OF BRITISH COLUMBIA

(Vancouver)

October 2013

Abstract

We study the evolution of a warm dark matter and perfect fluid system to determine its behaviour in the linear regime. Comparative analysis is performed between cold dark matter, hot dark matter and warm dark matter approximating each case. Numerical issues causes differences between the warm dark matter approximations and the respective case. Numerical issues that we have been unable to solve prevent the calculation of sufficient k-space modes to study interesting scales. Analytic methods to obtain the real space perturbations and distribution functions are derived.

Preface

For my Master's program, I was tasked with of solving the warm dark matter collapse problem, assigned to me by my supervisor, Dr Kris Sigurdson. In my research, my supervisor, and Dr Annika Peter, mainly helped by pointing me towards possible fixes for programming bugs I encountered, and suggesting literature to review, but overall, I was in charge of writting the code, finding the numerical problems, and fixing them. Once we obtained data, I was responsible for performing the analysis and determining what methods would be used, under the direction of my supervisor and Dr Peter.

None of the details of this thesis have been published.

Table of Contents

List of Figures

Acknowledgements

I would like to thank my supervisor, Dr Kris Sigurdson, for the advice and direction given during this thesis. I would also like to thank Dr Annika Peter for her help in problem solving and debugging the code. Thanks to Dr Douglas Scott for ensuring my thesis was properly formatted. I thank my parents for supporting me throughout my education. And lastly, I thank my fiance, Sam Snobelen, for pushing me to continue when things seemed bleak.

Chapter 1

Introduction

Understanding how planets, stars, galaxies formed has been a point of interest throughout history. With advances in general relativity, statistical mechanics and electromagnetism from the last century, we are now in a position to attempt to explain how these structures are formed. The current model used for structure formation is the ΛCDM model [3]. In this model, there exists the standard model particles, along with cold dark matter (CDM) and a cosmological constant, Λ, acting as dark energy. The presence of CDM and a cosmological constant in the model are due to observations that suggest that visible matter does not account for the all gravitational force observable in our Universe. In effect, visible matter accounts for only roughly 5% of all matter, with dark matter being approximately 27% and dark energy representing the remaining 68% [1]. In cosmology,"dark" signifies that there is no interaction with electro-magnetic force. [9] This translates to no photon production/absorption during interactions with dark matter/energy. This lack of interaction causes dark matter/energy to be elusive in nature, and their existence is inferred from gravitational interactions, which are much weaker then electro-magnetic interactions. The "cold" descriptor for cold dark matter relates to the matter's momentum. A cold particle exhibits a

small p/m ratio, where p is the momentum and m, the mass [9]. We will look at the detailed implications of this in further chapters, but in short, it causes many simplifications to the system. There has been much work done to understand how cold dark matter collapses to form structures [5][15][14][2][10]. This thesis will look at the effect of making the dark matter "warm". In this context, warm signifies particles for which p/m begins relatively large and becomes insignificant at late times [9]. Before we continue the discussion of warm dark matter (WDM) collapse, we will define some basic concepts in cosmology, and look at the collapse of CDM in more detail.

1.1 Cosmological Definitions

In the field of cosmology, time and distance are not uniquely defined quantities. There exist numerous different ways to measure both of these quantities [3]. For distances, the curvature of space-time itself and the expansion of the Universe cause some issues of definition. When considering expansion, distances measured today were not the same as in the past, and this change in distance is significant. In order to deal with this change, the scale factor, a, is defined. If a distance x is measured today, it is at a distance of ax at another time. This definition sets $a_0 = 1$, where the subscript 0 indicates today. As our Universe is expanding, distances were smaller in the past, and hence past values of a are smaller then 1 [3]. The exact behaviour of a is based on the composition of the Universe[3].

In order to find a definition of time, we must decide if we desire proper time or coordinate time[3]. Proper time is measured based on a comoving

observer, while coordinate time is measured by an outside observer. Let us consider the distance light can travel in an expanding universe since $t = 0$ from the view of a comoving observer. The velocity of light can be taken to be 1, as we are free to set $c = 1$. This choice of value for c gives us that $d/t = 1$. If we consider only an infinitesimal time step dt, we obtain $dt = a(t)dx$. As we wish to calculate the distance light has travelled we are interested in

$$\tau(t) = \int_{x(t=0)}^{x(t)} dx' = \int_0^t \frac{dt'}{a(t')}. \tag{1.1}$$

As dt and a are always positive, τ is an increasing function. This property makes τ an ideal candidate for a time variable. As a time coordinate, it is refered to as "conformal time"[3]. This qunatity contains some important information. As it represents the distance light has travelled, it also gives the maximum distance two objects can be apart to have been in causal contact in the past. We call this distance the "horizon"[3]. As will be seen later, we will be working in Fourier transformed k-space for much of our calculations. In k-space, modes for which $k\tau < 1$ have not yet crossed the horizon and these are called "super-horizon" modes, while those with $k\tau > 1$ are "sub-horizon" modes. These two ranges of k will have distinct behaviour, as we will see once we have derived the relevant equations for the evolution of k-modes.

1.2 Units

In this paper, we will be using only Mpc as units. In order to achieve this, we set the following constants to 1 : $c, k_B, \hbar$. In this system, quantites are usually expressed in terms of eV. We use G to change from eV to Mpc. The value of G in the appropriate units is $G = 163.9964\text{Mpc}^{-2}\text{eV}^{-4}$.

Chapter 2

Unperturbed System

We begin our study with an unperturbed universe. It is isotropic and homogeneous. All directions and all parts of space are the same. We will relax the homogeneous condition as we progress, as we need inhomogeneities in the matter distribution to cause matter to gravitationally collapse and produce the structure we see in the Universe. We will need to determine the metric to use, derive the general relativistic equations, and define the quantities of interest. Once this framework is built, we will add perturbations to it to eventually obtain our desired warm dark matter system.

2.1 Metric Defnitions

The metric contains information about the curvature of space-time. This is one of two components necessary to determine the general relativity equations, the other component being the stress-energy tensor. For an isotropic and homogeneous expanding Universe, the metric to use is[9]

$$ds^2 = -a^2 d\tau^2 + a^2 dx^i dx_i. \tag{2.1}$$

We use conformal time as our time variable. ds^2 is the proper distance

in space-time in this metric. Roman indices are used to sum over the spatial indices (1,2,3), while greek indices will also sum over the temporal indice (0). The metric may also be written as

$$ds^2 = g_{\mu\nu} dx^\mu dx^\nu. \tag{2.2}$$

We must work our way from this metric to solving for the Einstein tensor, $G_{\mu\nu}$:

$$G_{\mu\nu} \equiv R_{\mu\nu} - \frac{1}{2} g_{\mu\nu} \mathcal{R} = 8\pi G T_{\mu\nu}, \tag{2.3}$$

where, $R_{\mu\nu}$ is the Ricci tensor, $\mathcal{R}$ is the Ricci scalar and $T_{\mu\nu}$ is the stress-energy tensor[3]. We will go through the process of defining and deriving all these quantities for this system. We begin with

$$R_{\mu\nu} = \Gamma^\alpha_{\mu\nu,\alpha} - \Gamma^\alpha_{\mu\alpha,\nu} + \Gamma^\alpha_{\beta\alpha}\Gamma^\beta_{\mu\nu} - \Gamma^\alpha_{\beta\nu}\Gamma^\beta_{\mu\alpha}, \tag{2.4}$$

where $\Gamma^\mu_{\alpha\beta}$ is the Christoffel symbol, while the comma represents a derivative, for example $R_{,\alpha}$ is the derivative of R with respect to x^α[3]. The Christoffel symbol is defined as[3]

$$\Gamma^\mu_{\alpha\beta} = \frac{g^{\mu\nu}}{2}[g_{\alpha\nu,\beta} + g_{\beta\nu,\alpha} - g_{\alpha\beta,\nu}]. \tag{2.5}$$

Continuing our definitions,

$$\mathcal{R} \equiv g^{\mu\nu} R_{\mu\nu} \tag{2.6}$$

and

$$T^{\mu}_{\nu} = P g^{\mu}_{\nu} + (\rho + P) U^{\mu} U_{\nu}, \tag{2.7}$$

where $U^{\mu} = dx^{\mu}/\sqrt{-ds^2}$ is the four-velocity[9].

2.2 Metric Calculations

We now have all the pieces to solve the unperturbed system. We obtain the following Christoffel symbols :

$$\Gamma^{0}_{00} = \left(\frac{\dot{a}}{a}\right); \tag{2.8a}$$

$$\Gamma^{0}_{ij} = \Gamma^{i}_{0j} = \Gamma^{i}_{j0} = \delta^{i}_{j}\frac{\dot{a}}{a}. \tag{2.8b}$$

All other Γs are zero. Here the dot represents a derivative with respect to τ.

We now use the Christoffel symbols to obtain the Ricci tensor :

$$R_{00} = -3\frac{d}{d\tau}\frac{\dot{a}}{a}; \tag{2.9a}$$

$$R_{ij} = \delta_{ij}\left\{\frac{d}{d\tau}\left(\frac{\dot{a}}{a}\right) + 2\left(\frac{\dot{a}}{a}\right)^{2}\right\}. \tag{2.9b}$$

The other Ricci tensor coefficients are zero.

The Ricci scalar can now be calculated. We obtain

$$\mathcal{R} = \frac{6}{a^2}\left(\frac{\ddot{a}}{a}\right). \tag{2.10}$$

The stress-energy tensor, T^{μ}_{ν}, is the last piece we need. It is defined as

$$T^0_0 = -\rho, \tag{2.11a}$$

$$T^0_i = T^i_0 = 0, \tag{2.11b}$$

$$T^i_j = \delta^i_j P, \tag{2.11c}$$

where ρ and P are the energy density and the pressure, respectively.

It will be noted that we used a different configuration of indices for T^{μ}_{ν} then we used in the Einstein equation (2.3). This is done to avoid scale factors appearing into the stress-energy tensor. We will now need to change the Einstein tensor to this form in order to solve the Einstein equation. To change indices, we use $T^{\mu}_{\nu} = g_{\alpha\nu}T^{\mu\alpha}$.

After the change in indices, we obtain the final Einstein equations :

$$\left(\frac{\dot{a}}{a}\right)^2 = \frac{8\pi G}{3}a^2\rho; \tag{2.12}$$

$$\frac{d}{d\tau}\left(\frac{\dot{a}}{a}\right) = -\frac{4\pi G}{3}a^2(\rho + 3P). \tag{2.13}$$

We will redefine the energy density and pressure as follows $\rho' = \frac{8\pi G a^4}{3}\rho$ and $P' = \frac{8\pi G a^4}{3}P$, changing the above equations to

$$\dot{a} = \sqrt{\rho'}, \tag{2.14}$$

$$\frac{d}{d\tau}(\frac{\dot{a}}{a}) = -\frac{\rho' + 3P'}{2a^2}. \tag{2.15}$$

We may use these two equations to solve for $\dot{a}$, and correspondingly a. Once we have a, we know how the unperturbed universe evolves, solving it

completely. These equations are valid for a flat space-time. For a space-time that is positively or negatively curved, an additional term appears, modifying the first equation by the addition of a $-\kappa$ term. κ represents the overall curvature of space-time[3]. Hence, for a positively curved universe, $\kappa > 0$, and $\kappa < 0$ for a negatively curved universe. We will be mainly concerned with a universe with $\kappa = 0$ but the spherical collapse case will use $\kappa > 0$.

The next step in our derivation is to add perturbations to the energy-stress tensor and determine their evolution equations.

Chapter 3

Derivation from the Metric

There exists two common gauges used in cosmology for the evolution of perturbations, the synchronous gauge and the conformal Newtonian gauge.[9] In this thesis, the focus will be solely on the conformal gauge. This choice is made due to the physical interpretation of the conformal Newtonian gauge. The gravitational perturbation ψ is equivalent to the Newtonian gravitational potential, and as such, previous intuition can be used when analyzing the gravitational perturbation. It should be noted that the majority of the derivations in Chapters 3,4 and 5 fill in the details of the derivations from [9].

For the conformal Newtonian gauge, the perturbed metric equation can be written as [9]

$$ds^2 = a^2(\tau)\{-(1+2\psi)d\tau^2 + (1-2\phi)dx^i dx_i\}. \tag{3.1}$$

We may perform a similar analysis for this metric as was performed for the unperturbed state. The equation for the Einstein tensor can be decomposed as follows [3]:

$$G^\mu_\nu + \delta G^\mu_\nu = 8\pi G(T^\mu_\nu + \delta T^\mu_\nu). \tag{3.2}$$

As we have already solved the unperturbed parts, these will cancel, and we obtain

$$\delta G^{\mu}_{\nu} = 8\pi G \delta T^{\mu}_{\nu}. \tag{3.3}$$

This will prevent us from repeating the derivations of the unperturbed system.

From Ref. [7], the perturbed Christoffel symbols are:

$$\delta\Gamma^{0}_{00} = \dot{\psi}; \tag{3.4a}$$

$$\delta\Gamma^{0}_{0i} = \delta\Gamma^{0}_{i0} = \psi_{,i}; \tag{3.4b}$$

$$\delta\Gamma^{0}_{ij} = -\delta_{ij}\{2H(\phi+\psi) + \dot{\phi}\}; \tag{3.4c}$$

$$\delta\Gamma^{i}_{00} = \psi_{,i}; \tag{3.4d}$$

$$\delta\Gamma^{i}_{0j} = -\dot{\phi}\delta^{i}_{j}; \tag{3.4e}$$

$$\delta\Gamma^{i}_{jk} = (\phi_{,k}\delta^{i}_{j} + \phi_{,j}\delta^{i}_{j}) + \phi_{,i}\delta_{jk}. \tag{3.4f}$$

Having these perturbed Christoffel symbols, we can now calculate the perturbed Ricci tensor coefficients:

$$\delta R^{0}_{0} = a^{-2}\left\{-3\ddot{\phi} - \nabla^{2}\psi - 3\frac{\dot{a}}{a}(\dot{\psi}+\dot{\phi}) - 6\frac{d}{d\tau}\left(\frac{\dot{a}}{a}\right)\psi\right\}; \tag{3.5a}$$

$$\delta R^{0}_{i} = -2a^{-2}\left(\dot{\phi} + \frac{\dot{a}}{a}\psi\right)_{i} = -R^{i}_{0}; \tag{3.5b}$$

$$\delta R^{i}_{j} = a^{-2}\left[-\ddot{\phi} + \nabla^{2}\phi - \frac{\dot{a}}{a}(\dot{\psi}+2\dot{\phi}) - \left\{2\frac{d}{d\tau}\left(\frac{\dot{a}}{a}\right) + 4\left(\frac{\dot{a}}{a}\right)^{2}\right\}\psi\right]\delta^{i}_{j} + a^{-2}(\phi-\psi)_{,ij}. \tag{3.5c}$$

It should be noted that due to the nature of index raising/lowering, the perturbed portion of the Ricci tensor is $\delta g^{\mu\alpha} R_{\alpha\nu} + g^{\mu\alpha} \delta R_{\alpha\nu}$.

This now allows us to find the perturbed curvature scalar,

$$\mathcal{R} = a^{-2}\Bigg[-6\ddot{\phi} + 2\nabla^2(2\phi - \psi) - 6\frac{\dot{a}}{a}(\dot{\psi} + 3\dot{\phi}) - 12\left\{\frac{d}{d\tau}\left(\frac{\dot{a}}{a}\right) + \left(\frac{\dot{a}}{a}\right)^2\right\}\psi\Bigg]. \tag{3.6}$$

Using the metric for the conformal Newtonian gauge, (3.1), we can determine δT^{μ}_{ν} using (2.7):

$$\delta T^0_0 = -\delta\rho; \tag{3.7a}$$

$$\delta T^0_i = (\rho + P)v_i = -\delta T^i_0; \tag{3.7b}$$

$$\delta T^i_j = \delta P \delta^i_j + \Sigma^i_j; \qquad \Sigma^i_i = 0. \tag{3.7c}$$

We can now combine the perturbed equations in order to obtain our Einstein equations:

$$a^{-2}\left\{-2\nabla^2\phi + 6\frac{\dot{a}}{a}\dot{\phi} + 6\left(\frac{\dot{a}}{a}\right)^2\psi\right\} = a^{-2}3\delta\rho', \tag{3.8a}$$

$$-2a^{-2}\left(\dot{\phi} + \frac{\dot{a}}{a}\psi\right)_{,i} = -a^{-2}3(\rho' + P')v_i, \tag{3.8b}$$

$$a^{-2}\Bigg(\Bigg[2\ddot{\phi} + \nabla^2(\psi - \phi) + \frac{\dot{a}}{a}(2\dot{\phi} + 4\dot{\psi}) + \left\{4\frac{d}{d\tau}\left(\frac{\dot{a}}{a}\right) + 2\left(\frac{\dot{a}}{a}\right)^2\right\}\psi\Bigg]\delta^j_i + (\phi - \psi)_{,ij}\Bigg) = a^{-2}\left(\frac{1}{2}\delta P'\right) + \Sigma^j_i. \tag{3.8c}$$

The third equation in this set is rather cumbersome. We may decompose

it into the trace and traceless components. Before doing this, we will convert to momentum space via a Fourier transform. It will be simpler to decompose (3.8c) in momentum space, and we will also be working in this space once we add interactions, as in linear theory it will decouple our equations [3], thus it will be good exercise to convert our equations now. The primary effect of this is the conversion of $,i$ into $-ik_i$. This gives us $\nabla^2 = -k^2$. Also, since the k_i vectors are Euclidean constructs, you can interchange their indices freely[3]. Focusing only on (3.8c), we obtain

$$\begin{aligned} a^{-2}\Bigg(\Bigg[2\ddot{\phi} + k^2(\phi-\psi) + \frac{\dot{a}}{a}(2\dot{\phi}+4\dot{\psi}) + \Bigg\{4\frac{d}{d\tau}\left(\frac{\dot{a}}{a}\right) + \\ 2\left(\frac{\dot{a}}{a}\right)^2\Bigg\}\psi\Bigg]\delta_i^j - k_i k_j(\phi-\psi)\Bigg) = a^{-2}\left(\frac{1}{2}\delta P'\delta_i^j\right) + \Sigma_i^j. \end{aligned} \tag{3.9}$$

We will decompose this equation into two components, the trace and traceless parts. For the trace, $\delta_i^i \to 3$ and $k_i k_i \to k^2$. The trace is then

$$\begin{aligned} a^{-2}\Bigg(\Bigg[2\ddot{\phi} + k^2(\phi-\psi) + \frac{\dot{a}}{a}(2\dot{\phi}+4\dot{\psi}) + \Bigg\{4\frac{d}{d\tau}\left(\frac{\dot{a}}{a}\right) + 2\left(\frac{\dot{a}}{a}\right)^2\Bigg\}\psi\Bigg]3 \\ -k^2(\phi-\psi)\Bigg) = a^{-2}\left(\frac{3}{2}\delta P'\right) + \Sigma_i^i. \end{aligned} \tag{3.10}$$

Since Σ_i^j is defined as traceless, $\Sigma_i^i = 0$. Dividing both sides by $3a^{-2}$, we obtain

$$\begin{aligned} 2\ddot{\phi} + k^2(\phi-\psi) + \frac{\dot{a}}{a}(2\dot{\phi}+4\dot{\psi}) + \Bigg\{4\frac{d}{d\tau}\left(\frac{\dot{a}}{a}\right) + 2\left(\frac{\dot{a}}{a}\right)^2\Bigg\}\psi \\ -a^2\frac{k^2}{3}(\phi-\psi) = \delta P'. \end{aligned} \tag{3.11}$$

Now, we deal with the traceless component of (3.8c). We can accomplish this by applying the traceless operator $\hat{k_i}\hat{k_j} - \frac{1}{3}\delta_{ij}$ [3]:

$$\left(\hat{k_i}\hat{k_j} - \frac{1}{3}\delta_{ij}\right) k^i k^j (\phi - \psi) = \left(\hat{k_i}\hat{k_j} - \frac{1}{3}\delta_{ij}\right) \Sigma_i^j. \tag{3.12}$$

Let us define

$$(\rho + P)\theta = ik^j \delta T_j^0, \tag{3.13a}$$

$$(\rho + P)\sigma = \left(\hat{k_i}\hat{k_j} - \frac{1}{3}\delta_{ij}\right) \Sigma_j^i. \tag{3.13b}$$

Simplifying the left hand side, we obtain our final equation

$$\frac{2}{3}k^2(\phi - \psi) = 3(\rho' + P')\sigma. \tag{3.14}$$

For ease, we will now restate the four basic equations as

$$k^2\phi + 3\frac{\dot{a}}{a}\left(\dot{\phi} + \frac{\dot{a}}{a}\psi\right) = \frac{3}{2}\delta\rho', \tag{3.15a}$$

$$k^2\left(\dot{\phi} + \frac{\dot{a}}{a}\psi\right) = \frac{3}{2}(\rho' + P')\theta, \tag{3.15b}$$

$$\ddot{\phi} + \frac{\dot{a}}{a}(\dot{\phi} + 2\dot{\psi}) + \left\{2\frac{d}{d\tau}\left(\frac{\dot{a}}{a}\right) + \left(\frac{\dot{a}}{a}\right)^2\right\}\psi - \frac{k^2}{3}(\phi - \psi) = \frac{1}{2}\delta P', \tag{3.15c}$$

$$k^2(\phi - \psi) = \frac{9}{2}(\rho' + P')\sigma, \tag{3.15d}$$

where, $\theta = k^i v_i$[3].

This completes the main derivations for the evolution of the background

and gravitational perturbation quantities. In the subsequent chapter, we will derive the equations for the perturbations for various types of particles, but beforehand, we will solve a simple system, the perfect fluid.

Chapter 4

Perfect Fluid

Before continuing on to consider the effects of particle interactions on the evolution of matter, we will look at the simplest type of matter, a perfect fluid. A perfect fluid is defined solely by its energy density, ρ and pressure,P [9]. This simplifications allow us to solve the entire system using energy-momentum conservation.

In general relativity, this principle is embodied by the following [3]

$$T^{\mu\nu}_{;\mu} = \delta_\mu T^{\mu\nu} + \Gamma^\nu_{\alpha\beta} T^{\alpha\beta} + \Gamma^\alpha_{\alpha\beta} T^{\nu\beta} = 0, \tag{4.1}$$

where ; represents the covariant derivative, which means it is invariant under gauge transforms.[9] Looking at the perturbed part of these equations, we obtain the following 2 equations:

$$\dot{\delta} = -(1+w)(\theta - 3\dot{\phi}) - 3\frac{\dot{a}}{a}\left(\frac{\delta P}{\delta\rho} - w\right)\delta; \tag{4.2a}$$

$$\dot{\theta} = -\frac{\dot{a}}{a}(1-3w)\theta - \frac{\dot{w}}{1+w}\theta + \frac{\delta P/\delta\rho}{1+w}k^2\delta - k^2\sigma + k^2\psi; \tag{4.2b}$$

Here $w = P/\rho$.

We will not cover these derivations in detail here, but aside from a few minor details, they are fairly straightforward calculations. The two main

details that must be used to obtain them is that $\dot{\delta} = \frac{\dot{\delta\rho}}{\rho} - \frac{\delta\rho\dot{\rho}}{\rho^2}$, and that $\frac{\rho}{a^2} = \left(\frac{\dot{a}}{a}\right)^2$ using our units. Using these two substitutions, it should be an exercise in algebra to obtain the previous equations.

There are two types of perfect fluids that we will be interested in, $w = 1/3$ and $w = 0$ fluids. $w = 1/3$ fluids are radiation fluids while $w = 0$ fluids represent cold dark matter (CDM)[9]. A radiation fluid will be included in our system to keep matter-radiation equality near to that of our Universe. The CDM is being considered as a test case for high mass WDM.

For both of these perfect fluids, $\dot{w} = 0$ and $\sigma = 0$[9].

4.1 Radiation

Substituting $w = 1/3$ into (4.2), we obtain

$$\dot{\delta} = -(4/3)(\theta - 3\dot{\phi}), \tag{4.3a}$$

$$\dot{\theta} = k^2(\delta + \psi). \tag{4.3b}$$

If only this perfect radiation fluid is assumed to exist, and (3.15a) or (3.15b) are used to evolve ϕ, this set of equations has an analytic solution of the form [4]

$$\phi = \frac{9\phi_0}{(k\tau)^3}\left[\sqrt{3}\sin\left(\frac{k\tau}{\sqrt{3}}\right) - k\tau\cos\left(\frac{k\tau}{\sqrt{3}}\right)\right], \tag{4.4a}$$

$$\delta = \frac{6\phi_0}{(k\tau)^3}\left[2\sqrt{3}((k\tau)^2 - 3)\sin\left(\frac{k\tau}{\sqrt{3}}\right) - k\tau((k\tau)^2 - 6)\cos\left(\frac{k\tau}{\sqrt{3}}\right)\right], \tag{4.4b}$$

$$\theta = -\frac{3\sqrt{3}k\phi_0}{2(k\tau)^2}\left[2\sqrt{3}k\tau\sin\left(\frac{k\tau}{\sqrt{3}}\right) - ((k\tau)^2 - 6)\cos\left(\frac{k\tau}{\sqrt{3}}\right)\right], \tag{4.4c}$$

where ϕ_0 is the initial value of ϕ.

This set of analytic solutions will be used to verify the numerical accuracy of the code, in the special case where only the perfect fluid is present. As the system of interest will have WDM mixed in with the perfect radiation fluid, the actual solution will differ from this analytic solution.

4.2 Cold Dark Matter

Substituting $w = 0$ into (4.2), we obtain

$$\dot{\delta} = -\theta + 3\dot{\phi}, \tag{4.5a}$$

$$\dot{\theta} = -\frac{\dot{a}}{a}\theta + k^2\psi. \tag{4.5b}$$

Again, this set of equations will be used to verify the code for the high mass case, where we expect the WDM to behave like CDM.

Chapter 5

Derivation from the Boltzmann Equation

Having now determined how the background and the gravitational potential behaves, we must now derive the evolution of the matter. Although we are primarily concerned with WDM, a bottom-up approach was used to build the code, where we started with the simplest systems and added to them until we reached WDM. For this reason, we have covered the evolution of cold dark matter, and will now consider massless neutrinos and massive neutrinos, where massive neutrinos will be the basis for our WDM [9]. Before we begin to think about the evolution for a specific case of matter though, we need to examine the distribution function and the Boltzmann equation. It will be noted that this chapter is strongly based on Ref. [9].

The Boltzmann equation utilizes phase space, which is a six dimensional space, having 3 positions, x_i and 3 momenta, $P_i = mU_i$. The positions may be represented by x_i, but the momenta will need to be examined more closely.

In the conformal gauge, we have

$$P_i = (1-\phi)ap_i, \tag{5.1a}$$

$$P^i = -(1+\phi)a^3 p_i. \tag{5.1b}$$

Let us define the phase space distribution function as

$$f(x^i, P_j, \tau)dx^1dx^2dx^3dP_1dP_2dP_3 = dN, \tag{5.2}$$

where dN is the number of particles in the volume $dx^1dx^2dx^3dP_1dP_2dP_3$.

We will decompose the distribution function,f, into an unperturbed and first order component, as follows

$$f(x^i, P_j, \tau) = f_0(1 + \Psi(x^i, P_j, \tau)). \tag{5.3}$$

In our previous definition of P, the metric perturbation appeared. This would complicate many calculations, but we may replace P_j by $q_j \equiv ap_j$[9]. As q_j is not the conjugate momentum, due to the lack of the $(1-\phi)$ term, we will need to be careful when working with the energy-momentum tensor, and the volume element. The volume element becomes $dx^1dx^2dx^3dq_1dq_2dq_3(1-3\phi)$ to first order. We can also define the comoving energy as $\epsilon = \sqrt{q^2 + a^2m^2}$. As this is the energy measured by a comoving observer, it is related to P_0,

the energy component of the momentum four-vector, through

$$P_0 = -(1+\psi)\epsilon, \tag{5.4a}$$

$$P^0 = (1-\psi)a^{-2}\epsilon. \tag{5.4b}$$

Another desired modification is the separation of the magnitude of q from its direction. This can be easily accomplished with the following definition $q_j = qn_j$ where $n^i n_i = \delta^i_j$. Our phase space distribution now depends on the position, q, n_j and time.

The zeroth order distribution function, f_0 will be the Fermi-Dirac function for fermions(+) and Bose-Einstein for bosons (−). As the particles decouple while highly relativistic, $q \gg am$ in the distribution function, and as such, we may approximate ϵ as q in the distribution function only:

$$f_0(q) = \frac{g_{\rm s}}{h_P^3}\frac{1}{e^{q/k_B T_0} \pm 1} \tag{5.5}$$

where $g_{\rm s}$ is the number of spin degrees of freedom, h_P is the Planck constant, k_B is the Boltzmann constant, and is set to 1, and T_0 is the temperature today. For the remainder of the discussion, we will redefine ϵ, q and m as follows:

$$q \to \frac{q}{T_0}; \qquad m \to \frac{m}{T_0}; \qquad \epsilon \to \frac{\epsilon}{T_0}. \tag{5.6a}$$

This is the notation used by CLASS [8].

We may decompose the distribution function into a zeroth order and

higher order components:

$$f(x^i, q, n_j, \tau) = f_0(q)(1 + \Psi(x^i, q, n_j, \tau) + ...), \tag{5.7}$$

where Ψ represents the first order perturbation. We will ignore the higher order perturbations.

We have previously written the energy-momentum tensor in terms of the metric (2.7). We can also express it in terms of the distribution function

$$T_{\mu\nu} = \int dP_1 dP_2 dP_3 (-g)^{-1/2} \frac{P_\mu P_\nu}{P^0} f(x^i, P_j, \tau), \tag{5.8}$$

where g is the determinant of the $g_{\mu\nu}$. For the conformal gauge, $g = -a^8(1 - 6\phi + 2\psi)$. It should also be noted that, as discussed earlier, $dP_1 dP_2 dP_3 = T_0^3 dq_1 dq_2 dq_3 (1 - 3\phi)$.

Combining all of these in equation (5.8), we can obtain the energy-momentum tensor:

$$T_0^0 = -\left(\frac{T_0}{a}\right)^4 \int q^2 dq d\Omega \epsilon f_0(q)(1 + \Psi); \tag{5.9a}$$

$$T_i^0 = \left(\frac{T_0}{a}\right) \int q^3 dq d\Omega n_i f_0(q) \Psi; \tag{5.9b}$$

$$T_j^i = \left(\frac{T_0}{a}\right) \int q^3 dq d\Omega n_i n_j \frac{q}{\epsilon} f_0(q)(1 + \Psi). \tag{5.9c}$$

It becomes easy to split this energy-momentum tensor into perturbed and unperturbed components as the only first order quantity present is Ψ. Because there exists simplifications to the integrand for various types of matter, we will wait to determine equivalence between this equation and

the quantities from equation (3.7).

As Ψ depends on τ, its evolution must be determined. We will use the Boltzmann equation to calculate this. The Boltzmann equation is

$$\frac{Df}{d\tau} = \frac{\partial f}{\partial \tau} + \frac{dx^i}{d\tau}\frac{\partial f}{\partial x^i} + \frac{dq}{d\tau}\frac{\partial f}{\partial q} + \frac{dn_i}{d\tau}\frac{\partial f}{\partial n_i} = \left(\frac{\partial f}{\partial \tau}\right)_{\mathrm{C}}, \tag{5.10}$$

Where right hand side is a collision term. As we will be dealing with dark matter, this term will be 0 for all cases we are interested in.

There is one simplification that can be done immediately. Since only Ψ depends on n_i, $\frac{\partial f}{\partial n_i}$ is a first order quantity. Also, only the gravitational potentials, ψ and ϕ, may cause changes to n_i, and so $\frac{dn_i}{d\tau}$ is also a first order quantity, making the combined term a second order perturbaion[3]. As we are only interested in first order quantities, we may ignore this term.

We will now determine expression for $\frac{dx^i}{d\tau}$. Multiplying by $\sqrt{-ds^2}$ we obtain [3]

$$\frac{dx^i}{\sqrt{-ds^2}}\frac{\sqrt{-ds^2}}{d\tau} = \frac{P^i}{P^0}, \tag{5.11a}$$

$$= -(1+\psi+\phi)\frac{q}{\epsilon}. \tag{5.11b}$$

There is now only one term left to calculate, $\frac{dq}{d\tau}$. We will use the geodesic equation,[3]

$$P^0\frac{dp^\mu}{d\tau} + \Gamma^\mu_{\alpha\beta}P^\alpha P^\beta = 0. \tag{5.12}$$

Setting $\mu = 0$, we obtain

$$\frac{dq}{d\tau} = q\dot{\phi} + i\epsilon n_i k_i \psi. \tag{5.13}$$

Utilizing all of these terms, we can obtain our general expression for the Boltzmann equation:

$$\frac{\partial \Psi}{\partial \tau} + i\frac{q}{\epsilon}(\vec{k}\cdot\hat{n})\Psi + \frac{df_0}{dq}\frac{q}{f_0}\left[\dot{\psi} - i\frac{\epsilon}{q}(\vec{k}\cdot\hat{n})\psi\right] = 0. \tag{5.14}$$

It should be noted that the only dependance on $\hat{n}$ is through its dot product with $\vec{k}$. As only the angle between both terms is significant, we may set the direction of $\hat{n}$ and only consider the angle between both vectors.

There remains one more detail to iron out before utilizing equation (5.14). We must determine the k-space expression for Ψ. This will be done differently for the massless neutrino and massive neutrino cases that we will be considering,i.e. the hot dark matter, and warm dark matter candidates, respectively.

5.1 Massless Neutrinos

For massless neutrinos, $m = 0$, causing $\epsilon = q$. This causes massless neutrinos to be a type of hot dark matter (HDM) as they remain relativistic at all times. With this simplification, equations (5.9) and (3.7) may be used together to obtain expressions for ρ and P and their perturbations. We

obtain,

$$\rho = 3P = \left(\frac{T_0}{a}\right)^4 \int q^3 dq d\Omega f_0(q), \tag{5.15a}$$

$$\delta\rho = 3\delta P = \left(\frac{T_0}{a}\right)^4 \int q^3 dq d\Omega f_0(q)\Psi, \tag{5.15b}$$

$$\delta T^0_i = \left(\frac{T_0}{a}\right)^4 \int q^3 dq d\Omega n_i f_0(q)\Psi, \tag{5.15c}$$

$$\Sigma^i_j = \left(\frac{T_0}{a}\right)^4 \int q^3 dq d\Omega \left(n_i n_j - \frac{1}{3}\delta_{ij}\right) f_0(q)\Psi. \tag{5.15d}$$

We will integrate out the q dependance, and expand the angular dependence into a series of Legendre polynomials, $P_l(\hat{k}\cdot\hat{n})$

$$F(\vec{k},\hat{n},\tau) \equiv \frac{\int q^3 dq f_0(q)\Psi}{q^3 dq f_0(q)} \equiv \sum_{l=0}^{\infty}(-i)^l(2l+1)F_l(\vec{k},\tau)P_l(\hat{k}\cdot\hat{n}). \tag{5.16}$$

With this new definition, we have removed the dependance on q, and isolated the dependence on $\hat{n}$. Combining (5.15), (5.16) and (5.9), we may obtain

$$\delta = \frac{1}{4\pi}\int d\Omega F = F_0, \tag{5.17a}$$

$$\theta = \frac{3i}{16\pi}\int d\Omega k(\hat{k}\cdot\hat{n})F = \frac{3}{4}kF_1, \tag{5.17b}$$

$$\sigma = -\frac{3}{16\pi}\int d\Omega \left[(\hat{k}\cdot\hat{n})^2 - \frac{1}{3}\right] F = \frac{1}{2}F_2. \tag{5.17c}$$

It is now time to simplify the Boltzmann equation for the massless neutrinos. We can integrate (5.14) over $\int q^3 dq f_0(q)$ and divide by $\int q^3 dq f_0(q)$. The only term that is not evident is $\frac{\int \frac{d\ln f_0}{d\ln q} q^3 f_0 dq}{\int q^3 f_0 dq}$. Using integration by parts,

it can be shown that this term is equal to -4. With these, we obtain

$$\frac{\partial F}{\partial \tau} + ik\mu F = 4(\dot{\phi} - ik\mu\psi). \tag{5.18}$$

where $\mu = \hat{k} \cdot \hat{n}$.

Using the orthonormality of the Legendre polynomials, along with the recursion relation $\mu P_l(\mu) = \frac{1}{2l+1}((l+1)P_{l+1} + lP_{l-1})$, we may decompose (5.18) into individual moments to obtain

$$\dot{\delta} = -\frac{4}{3}\theta + 4\dot{\phi}, \tag{5.19a}$$

$$\dot{\theta} = k^2\left(\frac{1}{4}\delta - \sigma\right) + k^2\psi, \tag{5.19b}$$

$$\dot{F}_l = \frac{k}{2l+1}[lF_{l-1} - (l+1)F_{l+1}]. \tag{5.19c}$$

It should be noted that each mode is only coupled to the neighbouring modes. Also, we have now decoupled our single real space equation into an infinite set of harmonic equations. We will choose some maximum mode, $l_{\max}$, as a cutoff. We must be careful with this truncation though, as the incorrect $l_{\max+1}$ mode will affect $l_{\max}$ and then trickle down the hierarchy. In order to minimize this error, we will use the following recurrence relationship

$$F_{l_{\max}+1} = \frac{2l_{\max}+1}{k\tau}F_{l_{\max}} - F_{l_{\max}-1}, \tag{5.20}$$

which is inspired by the spherical Bessel behaviour exhibited by numerical solutions.[9]

We will choose to truncate at $l = 2000$, as is suggested in Ref. [9]. Much like

the CDM case will be a test for a high mass WDM, the massless neutrinos will be used as a test case for the low mass WDM.

5.2 Massive Neutrinos

Unlike with the massless neutrinos, the massive neutrinos do not allow for $q = \epsilon$, as $m \neq 0$. This allows for no simplifications of equation (5.9). Also, since ϵ depends on τ and q, we may not integrate over q. As such, we will expand Ψ itself as the following Legendre series

$$\Psi(\vec{k}, \hat{n}, q, \tau) = \sum_{l=0}^{\infty} (-i)^l (2l+1) \Psi_l(\vec{v}, q, \tau) P_l(\hat{k} \cdot \hat{n}). \tag{5.21}$$

Applying this expansion to (5.9), we obtain

$$\delta\rho = 4\pi \left(\frac{T_0}{a}\right)^4 \int q^2 dq \epsilon f_0(q) \Psi_0, \tag{5.22a}$$

$$\delta P = \frac{4\pi}{3} \left(\frac{T_0}{a}\right)^4 \int q^2 dq \frac{q^2}{\epsilon} f_0(q) \Psi_0, \tag{5.22b}$$

$$(\rho + P)\theta = 4\pi k \left(\frac{T_0}{a}\right)^4 \int q^3 dq f_0(q) \Psi_1, \tag{5.22c}$$

$$(\rho + P)\sigma = \frac{8\pi}{3} \left(\frac{T_0}{a}\right)^4 \int q^2 dq \frac{q^2}{\epsilon} f_0(q) \Psi_2. \tag{5.22d}$$

Using the properties of the Legendre polynomials, as with the massless

case, we may decouple the moments of Ψ in (5.14) as follows:

$$\dot{\Psi}_0 = -\frac{qk}{\epsilon}\Psi_1 - \dot{\phi}\frac{d\ln f_0}{d\ln q}; \tag{5.23a}$$

$$\dot{\Psi}_1 = \frac{qk}{3\epsilon}(\Psi_0 - 2\Psi_2) - \frac{\epsilon k}{3q}\psi\frac{d\ln f_0}{d\ln q}; \tag{5.23b}$$

$$\dot{\Psi}_l = \frac{qk}{(2l+1)\epsilon}(l\Psi_{l-1} - (l+1)\Psi_{l+1}), \qquad l \geq 2. \tag{5.23c}$$

As with the massless case, a truncation is necessary. We will use

$$\Psi_{\nu(l_{\max}+1)} = \frac{(2l_{\max}+1)\epsilon}{qk\tau}\Psi_{\nu l_{\max}} - \Psi_{\nu(l_{\max}-1)}. \tag{5.24}$$

We may trunctate at a much lower value of l than in the massless neutrino case. This is due to the fact that the massive neutrinos will become non-relativistic, causing high multipole moments to decay rapidly. We choose $l = 50$, as suggested by [9].

Chapter 6

Initial Conditions and Normalization

Now that we have derived all the equations to evolve, we must determine the initial conditions. The first step in this process is to define a starting point for the simulation. At early times, during the radiation domination, $\tau = \frac{a}{\dot{a}}$. We can see this fact by looking at equation (2.14). $\rho \propto a^{-4}$ for a radiation dominated Universe. As such, $\dot{a}$ is constant. Hence, $a = \dot{a}\tau$, giving us that $\frac{a}{\dot{a}} = \tau$.[9]

We set a such that our WDM begins radiation dominated, and use equation (2.14) to calculate $\dot{a}$. From equation (2.14), we also obtain that $(\frac{\dot{a}}{a})^2 = \tau^{-2} = \frac{\rho}{a^2}$. The value of τ obtained must also satisfy $k\tau \ll 1$. Additionally, since our WDM is radiation dominated, we may treat it as a massless neutrino at early times.

There exists some freedom in choosing an initial condition. For a detailed description on the different options, see Ref. [7]. We choose the adiabatic initial conditions for our case. This means that we set entropy perturbations to 0. This is a similar case to the analytic solution in equation (4.4) that we studied earlier. By examining those solutions, we find that $\dot{\phi} = \dot{\psi} = 0$.

We can use this, along with our early time details from earlier to transform equation (3.15), (4.3) and (5.19) into

$$k^2\phi + \frac{3}{\tau^2}\psi = -\frac{3}{2}\rho\delta, \tag{6.1a}$$

$$\frac{k^2}{\tau}\psi = 2\rho\theta, \tag{6.1b}$$

$$k^2(\phi - \psi) = 6\rho\sigma, \tag{6.1c}$$

$$\dot{\delta}_{\text{wdm}} = \dot{\delta}_{\text{pf}} = -\frac{4}{3}\theta, \tag{6.1d}$$

$$\dot{\theta}_{\text{wdm}} = k^2\left(\frac{1}{4}\delta_{\text{wdm}} - \sigma_{\text{wdm}} + \psi\right), \tag{6.1e}$$

$$\dot{\theta}_{\text{pf}} = k^2\left(\frac{1}{4}\delta_{\text{pf}} + \psi\right), \tag{6.1f}$$

$$\dot{\sigma}_{\text{wdm}} = \frac{4}{15}\theta, \tag{6.1g}$$

where wdm and pf are used to denote the WDM and the perfect fluid cases, respectively. Also, substituting $\rho = \tau^{-2}$ into (6.1), and ignoring the $(k\tau)^2$ factors, we obtain

$$-2\psi = \delta, \tag{6.2a}$$

$$\frac{k^2\tau}{2}\psi = \theta, \tag{6.2b}$$

$$\frac{k\tau^2}{6}(\phi - \psi) = \sigma, \tag{6.2c}$$

$$\dot{\delta}_{\text{wdm}} = \dot{\delta}_{\text{pf}} = -\frac{4}{3}\theta, \tag{6.2d}$$

$$\dot{\theta}_{\text{wdm}} = k^2\left(\frac{1}{4}\delta_{\text{wdm}} + \psi\right), \tag{6.2e}$$

$$\dot{\theta}_{\text{pf}} = k^2\left(\frac{1}{4}\delta_{\text{pf}} + \psi\right), \tag{6.2f}$$

$$\dot{\sigma}_{\text{wdm}} = \frac{4}{15}\theta_{\text{wdm}}. \tag{6.2g}$$

We have removed the $\sigma_{\rm wdm}$ term from equation (6.2d) as it is proportional to $(k\tau)^2$ as seen from equation (6.2c). We can see from these equations, that $\dot{\delta}_{\rm wdm}$ and $\dot{\delta}_{\rm pf}$ follow the same evolution. The same can be said about the θ equations. With this, we know that $\delta_{\rm wdm} = \delta_{\rm pf}$ and $\theta_{\rm wdm} = \theta_{\rm pf}$. We must relate δ to $\delta_{\rm wdm}$ and $\delta_{\rm pf}$, and similarly for θ and σ. This is done through

$$\delta = (1 - R_{\rm wdm})\delta_{\rm pf} + R_{\rm wdm}\delta_{\rm wdm}, \tag{6.3a}$$

$$\theta = (1 - R_{\rm wdm})\theta_{\rm pf} + R_{\rm wdm}\theta_{\rm wdm}, \tag{6.3b}$$

$$\sigma = R_{\rm wdm}\sigma_{\rm wdm}, \tag{6.3c}$$

where

$$R_{\rm wdm} = \frac{\rho_{\rm wdm}}{\rho_{\rm wdm} + \rho_{\rm pf}}. \tag{6.4}$$

We see from these, that if $\delta_{\rm wdm} = \delta_{\rm pf}$, $\delta = \delta_{\rm pf}$. The same holds for θ. We now have expressions for δ and θ. We wish to find an expression for σ now. Let us consider equation (6.2g). If we substitute our result from equation (6.2b) and integrate over τ, we obtain

$$\sigma_{\rm wdm} = \frac{(k\tau)^2}{15}. \tag{6.5}$$

Using this with equations (6.3c) and (6.2c), we obtain

$$\phi = (1 + R_{\rm wdm})\psi. \tag{6.6}$$

We have now expressed all quantities of interest in terms of ψ. As we

are working in the linear regime, we are free to choose an initial value of ψ. We will choose $\psi = -\frac{1}{2}$, such that $\delta = 1$ initially.

Although we have all physical quantities determined, we need to find initial conditions for Ψ_l in order to evolve our WDM past the radiation dominated domain. To do this, we will observe the evolution equations for the moments. These reduce to

$$\dot{\Psi}_0 = -\frac{qk}{\epsilon}\Psi_1, \tag{6.7a}$$

$$\dot{\Psi}_1 = \frac{qk}{3\epsilon}(\Psi_0 - 2\Psi_2) - \frac{\epsilon k}{3q}\psi\frac{d\ln f_0}{d\ln q}, \tag{6.7b}$$

$$\dot{\Psi}_2 = \frac{qk}{5}(2\Psi_1). \tag{6.7c}$$

Again, we will ignore the second moment in $\dot{\Psi}_1$, as it is proportional to $(k\tau)^2$. We know that at early time, when $am \ll q$, $\epsilon = q$. This allows us to rewrite equation (5.22a) as

$$\delta_\nu = \frac{\int q^3 f_0(q)\Psi_0 dq}{\int q^3 f_0(q) dq}. \tag{6.8}$$

When deriving the massless neutrino case, we saw that if there was a factor of $\frac{d\ln f_0}{d\ln q}$, the integral fraction would simplify to -4. We can see that

$$\Psi_0 = -\frac{1}{4}\delta_{\rm wdm}\frac{d\ln f_0}{d\ln q} \tag{6.9}$$

satisfies the integral equation. Putting this solution into our evolution equa-

tions, we obtain the following [9]:

$$\Psi_1 = -\frac{\epsilon}{3qk}\theta_{\rm wdm}\frac{d\ln f_0}{d\ln q}; \tag{6.10a}$$

$$\Psi_2 = -\frac{1}{2}\sigma_{\rm wdm}\frac{d\ln f_0}{d\ln q}. \tag{6.10b}$$

With these initial conditions, we have all the necessary initial conditions for the WDM+pf system we will be interested in, but we need to determine the initial conditions for the CDM case.

For the pure CDM case, we begin with a matter dominated universe, which gives us $\frac{\dot{a}}{a} = 2\tau^{-1} = \rho^{1/2}$. There are only three variables to solve for in the CDM system, ψ, δ, θ, since $\phi = \psi$. We will begin our derivation of the initial conditions by rewritting our equations, and substituting in our value for $\frac{\dot{a}}{a}$. This gives us the following set of equations:

$$k^2\phi + \frac{12}{\tau^2}\psi = -\frac{3}{2}\rho\delta; \tag{6.11a}$$

$$\frac{2k^2}{\tau}\psi = \frac{3}{2}\rho\theta; \tag{6.11b}$$

$$\phi = \psi; \tag{6.11c}$$

$$\dot{\delta}_{\rm cdm} = -\theta_{\rm cdm}; \tag{6.11d}$$

$$\dot{\theta}_{\rm cdm} = -\frac{2}{\tau}\theta_{\rm cdm} + k^2\psi; \tag{6.11e}$$

Here we set $\dot{\phi} = \dot{\psi} = 0$, as in the WDM case.

By substituting $\rho = \frac{4}{\tau^2}$, and eliminating terms proportional to $(k\tau)^2$, we

obtain

$$\delta_{\rm cdm} = -2\psi, \tag{6.12a}$$

$$\theta_{\rm cdm} = k^2\tau\frac{\psi}{3}. \tag{6.12b}$$

We now have our CDM initial conditions. We are again free to set an initial value for ψ.

When we run a high mass WDM case, we will need initial conditions for Ψ_l. We will follow a similar derivation of these as in the radiation dominated WDM. The main difference exists in the integral performed over q to obtain δ. Where we previously multiplied by $q^3 f_0 dq$ before integrating, we now multiply by $amq^2 f_0 dq$. The difference is due to the estimate that was previously $\epsilon = q$, but now is $\epsilon = am$. By performing this new integral and dividing by ρ as before, we obtain -3 instead of -4. This gives us

$$\Psi_0 = -\frac{1}{3}\delta_{\rm cdm}\frac{d\ln f_0}{d\ln q}, \tag{6.13a}$$

$$\Psi_1 = -\frac{\epsilon}{3qk}\theta_{\rm cdm}\frac{d\ln f_0}{d\ln q}, \tag{6.13b}$$

$$\Psi_2 = 0. \tag{6.13c}$$

This concludes the derivation of the initial conditions. We may now begin discussing details of the numerical routines to be used to solve the equations derived.

Chapter 7

Numerical Details

There are two major numerical elements that must be discussed here, the values to be used for the energy densities, and the numerical routines utilized during the simulation.

It should be noted at this point that we have not defined what our perfect fluid or WDM will consist of, namely, we have not determined what f_0 is for either component. For the WDM, we will choose

$$f_0(q) = \frac{g_s}{(2\pi)^3}\frac{1}{e^q + 1}, \tag{7.1}$$

while the perfect fluid will be

$$f_0(q) = \frac{3}{(2\pi)^3}\frac{1}{e^q + 1} + \frac{1}{(2\pi)^3}\frac{1}{e^q - 1}. \tag{7.2}$$

The perfect fluid distribution function is made to represent a mix of photons and neutrinos, while the WDM distribution is chosen to be comparable to the massive neutrino case studied earlier.

7.1 Energy Density Normalization

Normally $g_{\rm s}$ represents the number of degrees of freedom, but since we are not specifying a specific WDM candidate, we shall leave $g_{\rm s}$ as a free parameter, giving us the freedom to set $\rho_{\rm wdm}$ to a desirable quantity. Looking at our equations, the only time the factor of $g_{\rm s}$ will appear will be in conjecture with $T^4_{\rm 0wdm}$. As this is also the only time $T_{\rm 0wdm}$ explicitly enters the equations due to our scaling, this allows us to set the full product of $g_{\rm s}T^4_{\rm 0wdm}$ to determine the density. As we are not setting a specific value for $T_{\rm 0wdm}$, we will need to set $\frac{m}{T_{\rm 0wdm}}$ instead of m.

For the perfect fluid, we shall consider a mix of fermions and bosons. From Ref. [3], we can determine that

$$\rho_{\rm pf} = \frac{\pi^2}{15}\left\{1 + 3\left(\frac{7}{8}\right)\left(\frac{4}{11}\right)^{4/3}\right\}T^4_{\rm pf}. \tag{7.3}$$

We have assumed that the fermions are massless neutrinos and that the bosons are photons. This is done to attempt to simulate the real Universe. With this goal in mind, we shall also set $\rho_{\rm crit}$ to be that seen in the real niverse. We will also set $\rho_{\rm pf}/\rho_{\rm wdm}$ at $a = 1$ to be equal to the $\rho_{\rm rad}/\rho_{\rm matter}$ observed.

Using the radiation to matter ratio and the critical density, we may determine $\rho_{\rm pf}$ and $\rho_{\rm wdm}$ and use these to determine $T_{\rm 0pf}$ and $g_{\rm s}T^4_{\rm 0wdm}$. For the perfect fluid, we use equation (7.3), and for the WDM, we compare $\rho_{\rm wdm}$ with $4\pi g_{\rm s}(\frac{T_{\rm 0wdm}}{a})^4 \int q^2 dq\epsilon f_0(q)/g_{\rm s}$. We have now discussed how to set up the system and the equations that will be evolved within it.

7.2 Numerical Routines

There are two primary numerical calculations that are accomplished by the simulation, solving the differential equations and performing the integrals. For the differential equation solver, a Runge-Kutta routine will be used, with adaptive step size. We will use the routine odeint to drive the solver. For more details on these routines consult Ref. [12].

For the integration routine, we will use the Gauss-Laguerre quadrature routine described in Ref. [8]. This is a routine that works well for exponentially decaying functions that must be integrated from 0 to ∞. The basic quadrature expression is

$$I = \int_0^\infty dq f_0(q) g(q) \backsimeq \sum_{i=1}^{n} W_i g(q_i). \tag{7.4}$$

For the Gauss-Laguerre quadrature, we have this basic expression

$$\int_0^\infty dq e^{-q} h(q) \backsimeq \sum_{i=1}^{n} w_i h(q_i), \tag{7.5}$$

where q_i are the ith roots of L_n, the nth Laguerre polynomial. The weights w_i are determined from

$$w_i = \frac{q_i}{(n+1)^2 [L_{n+1}(q_i)]^2}. \tag{7.6}$$

If we set $h(q) = e^q f_0(q) g(q)$, we may relate w_i to W_i through

$$W_i = w_i e^{q_i} f_0(q_i). \tag{7.7}$$

This allows us to calculate the weights once for a set of q values, and then multiply them by the appropriate function g, depending on the integral. Another advantage of this routine is that one only needs a few q modes to obtain suitable precision. We choose to use 20 q modes for our case, as this leads to convergence.

Using both of these numerical routines, it is now possible to run the simulation, and obtain results.

Chapter 8

Simulation Results

Before looking at out results for the full simulation of the WDM+pf model, we will run the checks that have been discussed in previous chapters. We will verify first that the perfect fluid matches the analytic solution. We will then compare the high mass WDM to the CDM cases and the low mass WDM to the massless neutrino solution.

8.1 Perfect Fluid Comparison

We will be comparing the results from our numerical analysis and the analytic solution, (4.4).

We can see from Fig. 8.1 that there is no noticeable difference between both analytic and numerical solutions in the pure perfect fluid case at late times. When $k\tau \ll 1$, numerical issues cause the analytic solution to be inaccurate, but our computed solution matches with the expected value for the analytic solution. Once $k\tau$ becomes larger, there is a perfect match between both cases. As the analytic solution is only valid for a radiation dominated universe, we will not be able to use the analytic solution for the WDM+pf system once there is a significant matter component.

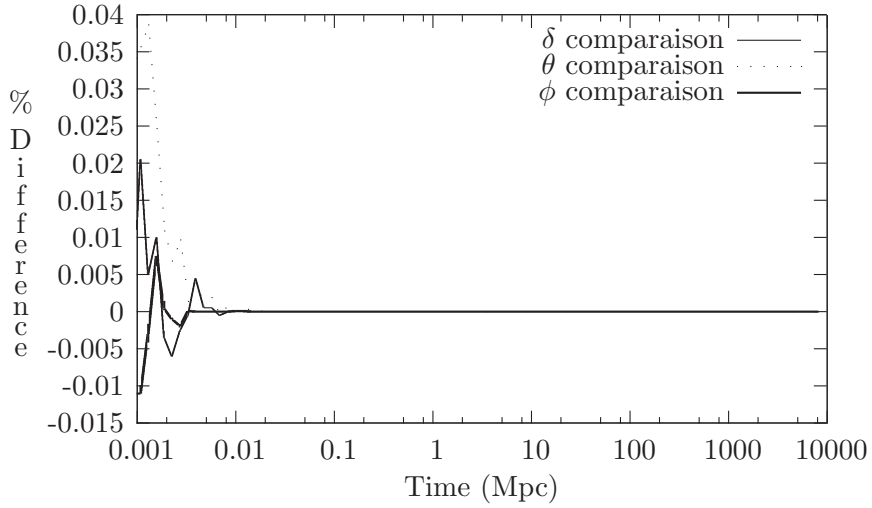

Figure 8.1: Perfect fluid comparison: Percentage difference between the analytic solution and numerical solution for a perfect fluid. At early times, the solution does not match, but this is due to the numerical issues when evaluating the analytic solution when $k\tau \ll 1$.

8.2 Cold Dark Matter Comparison

Having now confirmed that the perfect fluid component is properly calculated, we will now focus on making sure that the WDM component is working properly. We will begin with comparing a very high mass WDM scenario with the CDM case. We choose our mass such that the particles are non-relativistic at the start of the simulation. In order for both these cases to be comparable, we must evolve the high mass WDM alone, without the perfect fluid component. This ensures that we are in a matter dominated universe.

We can see from Fig. 8.2 that there are numerical differences between both cases. The difference remains small during the time of integration. The

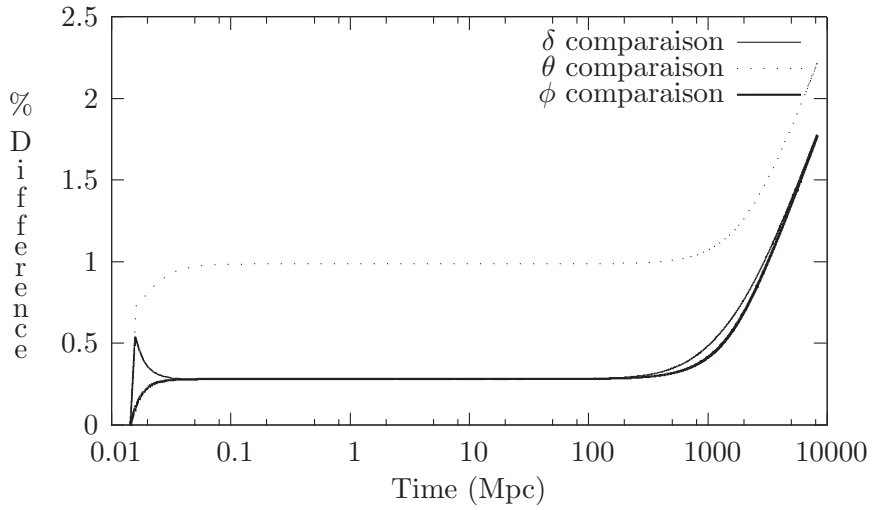

Figure 8.2: High mass warm dark matter comparison: Percentage difference between CDM and WDM with $m/T_0 = 10^{15}$. At early times, the difference is caused by a numerical inaccuracy in the integral to determine δ. At late times, the inaccuracy grows. The magnitude of the difference remains small for during the time of interest.

error is caused by the Laguerre quadrature integration method being inaccurate. One possible cause of this inaccuracy are the roots of the Laguerre polynomials used to calculate the weights. The values obtained through using the Gnu Scientific Library (GSL) Laguerre routine do not agree with the ones from Mathematica.[16] The values from the GSL routine matched the roots found when using the recursion relation,

$$\begin{aligned} L_0(x) &= 1, \\ L_1(x) &= 1 - x, \\ L_(k+1)(x) &= \frac{1}{1+k}((2k+1-x)L_k(x) - kL_{k-1}(x)). \end{aligned} \tag{8.1}$$

Hence the GSL roots were used. It is possible that the GSL routine uses the same recursion relation and that the same numerical inaccuracies appeared, causing both sets of roots to match, and causing the Mathematica roots to be the proper solution.

Another possible cause for the inaccuracy, is the number of moments present. In the CDM case, only the first two modes are considered as the others should be 0. When evolving the WDM case, there is the possibility of power leaking into higher moments as we do not automatically set them to 0. Even when setting the WDM case to only have 2 moments, there are similar innacuracies. Without having precise integration methods, it is hence difficult to judge if there are significant errors introduced by power leakage.

There now remains only one more area where the code may not be functional. We must now look at the low mass extreme limit.

8.3 Massless Neutrino Comparison

We will now look at the final test case, the low mass WDM. This regime should behave like the massless neutrino case. In order to make sure that our WDM has low enough mass, we set $\frac{m}{T_0} \ll 1$. This ensures that $\epsilon \sim q$.

It should be noted that Fig. 8.3 shows the actual difference and not percentile difference like the other plots. This is due to the oscillatory nature of the solution causing division by 0 if we tried to plot a relative difference.

From Fig. 8.3, we see a good match between both cases at early times, given that δ varies between -2 and 3, while ϕ is always between -1 and

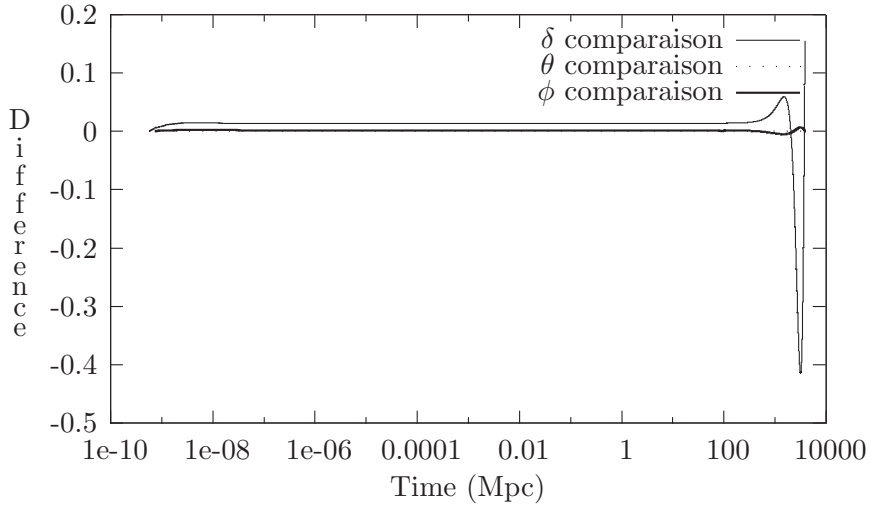

Figure 8.3: Low mass dark matter, absolute difference: Difference between massless neutrinos and WDM with $m/T_0 = 10^{-9}$. At early times, both cases are seen to agree, but as $k\tau > 1$, these cases start diverging.

1, and θ oscillates between -0.0015 and 0.0025. Both cases start diverging when $k\tau > 1$. The integration method does not always perform the best around origin crossing, due to the convergence check relying on the value itself. As our solution crosses 0, the integrator may be causing numerical inaccuracies, but it is difficult to ascertain due to the large number of equations, causing numerical issues difficult to track. Another possible source of inaccuracy is the number of moments present. As the low mass WDM needs to be solved for an array of q modes, it was not computationally feasible to solve it for the recommended 2000 modes or more with the equipment I had access to. As such, there may be power reflecting back to the lower moments instead of propagating.

8.4 Warm Dark Matter Data

Although some results from our simulation may be questionable, we will nevertheless perform the WDM+pf simulation. We choose m such that $am \ll q$ initially, but such that $m \gg q$. The behaviour of the solution will depend on the properties of the system when the modes cross the horizon, which occurs when $k\tau = 1$. Hence, small values of k will enter the horizon when $\epsilon \sim am$, and resemble CDM, while large k modes will cross when $\epsilon \sim q$, behaving like massless neutrinos when crossing the horizon. Since am will eventually dominate ϵ, we expect it will begin behaving like CDM at late times, but with a diminished amplitude, due to the decay present during the transition between the HDM and CDM regimes. The differential equation solver does not seem to converge when the modes cross while still in the HDM regime, or nearing transition to the CDM regime. As such, we may only look at purely CDM modes, and modes that transition to CDM shortly after horizon crossing. We will see the behaviour of the low k modes in Figs. 8.4, 8.5 and 8.6, where we look at the perturbations for a number of different k values.

Current versions of the code have difficulty with large k modes. We are limited to $k < 3\text{Mpc}^{-1}$ as this is the highest mode that will complete its evolution. Also, it should be noted that increasing values of k takes increasing time to calculate. The inaccuracies mentioned earlier may cause errors to accumulate, causing convergence of the differential equations to be slower and to also eventually cause the system to stop converging.

Once the numerical issues are solved, we may transform the k space data

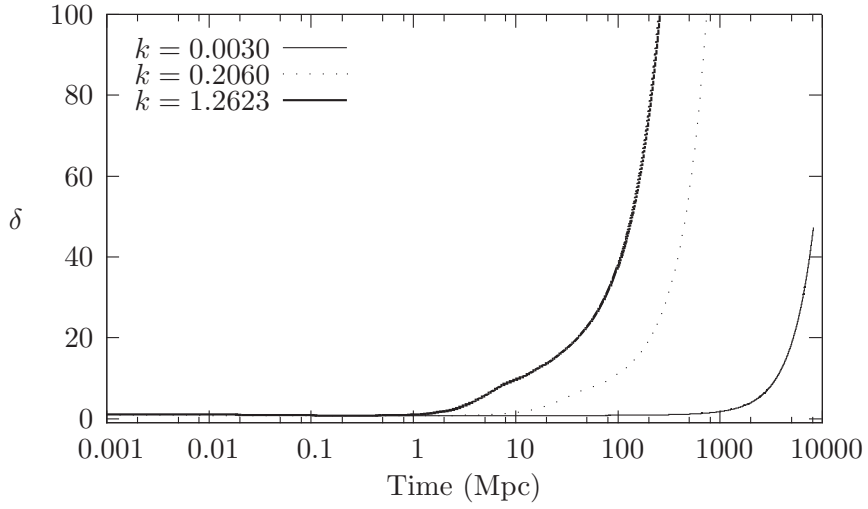

Figure 8.4: Warm dark matter: Evolution of δ for $k = 0.0030$ Mpc^{-1}, $k = 0.2060$ Mpc^{-1}, and $k = 1.2623$ Mpc^{-1} with $m/T_0 = 10^7$. We see that these modes lead to an increasing amlitude as expected.

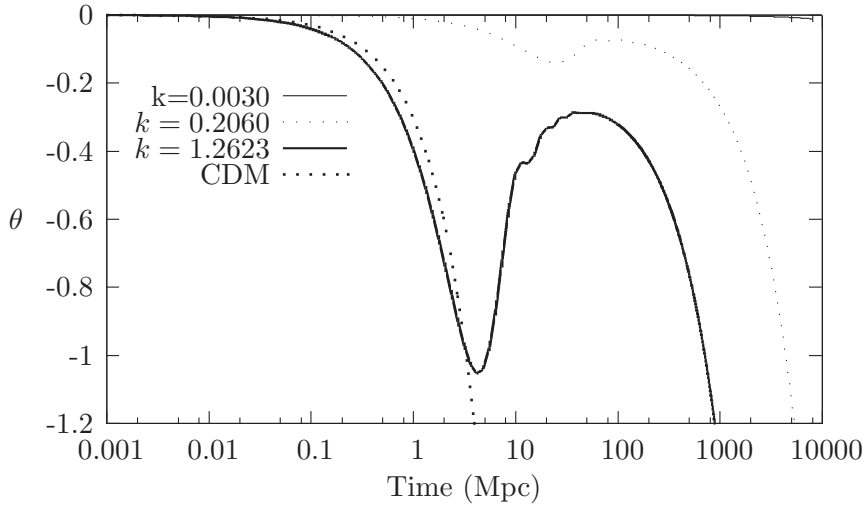

Figure 8.5: Warm dark matter: Evolution of θ for $k = 0.0030$ Mpc^{-1}, $k = 0.2060$ Mpc^{-1}, and $k = 1.2623$ Mpc^{-1} with $m/T_0 = 10^7$. We see that the higher k modes are not pure CDM. The increase in θ shortly after $k\tau = 1$ represents the momentum of the particles inhibiting the collapse of the system, as HDM would.

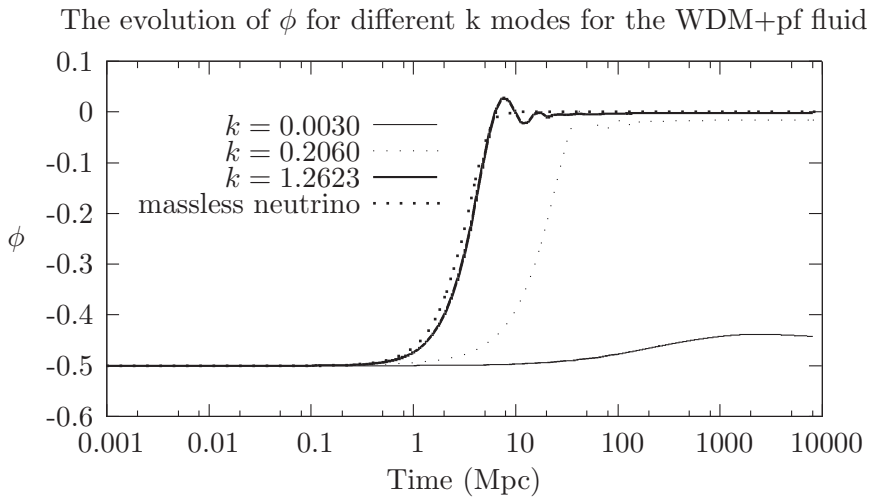

Figure 8.6: Warm dark matter: Evolution of ϕ for $k = 0.0030$ Mpc^{-1}, and $k = 0.2060$ Mpc^{-1}, $k = 1.2623$ Mpc^{-1} with $m/T_0 = 10^7$. For the larger k mode, we see some oscillations after horizon crossing. These are due to the presence of some mass as seen when comparing with the smooth massless neutrino case.

into real space to see how the WDM is collapsing. In the following chapter, we will discuss how we perform this real space transform.

Chapter 9

Data Analysis Routines

There are two different real space transforms that we wish to look at. We will begin by examining δ and θ in real space. Afterwards, we will look at the distribution functions in real space. We may use the information obtained from the perturbations to verify the distribution function.

9.1 Transfer Function

There is one important detail that has not been discussed yet that will allow us to perform these transforms. Upon looking at the equations that we evolve, all terms are proportional, to first order, to a perturbation. As such, we may multiply all the perturbations by some function of k, without affecting the equations. What this allows us to do is rewrite our perturbations as $T(k)F(k)$, where $T(k)$ is the quantity calculated in the previous sections $(\delta, \theta, \psi, \text{etc})$ and called the transfer function and $F(k)$ is some function of k[3]. We should note that despite $T(k)$ being different for each perturbation, $F(k)$ must be the same for all perturbations. What this decomposition allows us to do is set the initial distribution of matter. Since δ is constant at early times for all k, if we set $F(k)$ to the Fourier transform of some $f(x)$, $\delta(x, \tau_0)$ will have the same shape as $f(x)$. We may also use $F(k)$ to set the

properties of our system. By modifying the magnitude of $F(k)$, this will allow us to set either the magnitude of our initial conditions, or fix some end point quantity to a desired value. In our case, we chose to set σ_8, the RMS overdensity in a sphere of 8 Mpc[9], such that it was comparable with the real Universe, where

$$\sigma_8^2 = \langle \left[\frac{d^3k}{(2\pi)^3} \delta(\vec{k}) W_8(\vec{k}) \right]^2 \rangle, \tag{9.1}$$

where $W_8(\vec{k})$ is the Fourier transformed 3 dimensional top hat function for a 8 Mpc sphere.

9.2 Real Space Perturbations

We can now discuss the real space perturbations. We wish to work in three dimensional real space. Usually a Fast Fourier Transform (FFT) algorithm is used to numerically calculate Fourier transforms. Although these can be adapted to work in more then one dimension, we instead use the fact that our system is spherically symmetric to utilize a Hankel transform[11]. The Hankel transform is similar to a Fourier transform but it utilizes the Bessel functions as a basis instead of the complex exponential. The Hankel transform is also only valid for functions which only depend on r, whether it be in two dimensions or three. The transform is defined as [11]

$$H_\nu(k) = \int_0^\infty h(r) J_\nu(kr) r dr, \tag{9.2}$$

where J_ν is the Bessel function of first kind of order ν, with $\nu \geq -1/2$. The inverse is simply

$$h(r) = \int_0^\infty H_\nu(k) J_\nu(kr) k dk. \tag{9.3}$$

The integer values of ν represent the 2D transforms while the half integers are the 3D transforms. These are the ones we are interested in. We will be looking at the $\nu = 1/2$ transform. The corresponding Bessel function is

$$J_{1/2}(kr) = \sqrt{\frac{2kr}{\pi}} \frac{\sin(kr)}{kr}. \tag{9.4}$$

We cannot simply Hankel transform our calculated values with equation (9.3) as our transfer functions where specifically calculated in Fourier space. As such, we wish to equate the Fourier transform to the Hankel transform. We will use $f(r)$ and $F(k)$ to denote the Fourier functions, and $h(r)$ and $H_\nu(k)$ for the Hankel functions. If we perform the Fourier transform for a radially symmetric system, we obtain

$$F(k) = 4\pi \int_0^\infty f(r) \frac{\sin(kr)}{kr} r^2 dr. \tag{9.5}$$

Comparing $F(k)$ to $H_{1/2}(k)$, we can see that if we set

$$h(r) = f(r)(2\pi)^{3/2} \frac{\sqrt{r}}{\sqrt{k}}, \tag{9.6}$$

then both $F(k)$ and $H_{1/2}(k)$ are equal. The same analysis can be done for the inverse transforms, where we find that we must take the inverse of r and k to obtain equivalence.

There is one subtlety that we now must consider before applying this procedure to θ. When calculating θ, we used the fact that in Fourier space, the divergence in real space can be replaced by $-ik$ in Fourier space. This is a property of the Fourier transform and does not hold for the Hankel transform. As such, we must obtain a new method of transforming $\theta(k)$ using the Hankel transform. Beginning with the inverse Fourier transform, using the substitution procedure derived above, we will take the divergence on both sides to obtain

$$\nabla_r \cdot \vec{v}(r) = 4\pi \int_0^\infty \nabla_r \cdot (\vec{v}(k) \frac{\sin(kr)}{kr} k^2 dk). \tag{9.7}$$

Performing the derivative on the RHS, we obtain

$$\theta(r) = 4\pi \int_0^\infty v(\vec{k}) \left(\frac{\sin(kr)}{kr^2} + \frac{\cos(kr)}{r} \right) k^2 dk. \tag{9.8}$$

We can compare this expression with $J_{3/2}$ and $J_{1/2}$ to see that

$$\theta(r) = (2\pi)^{3/2} \int_0^\infty \frac{v(k)\vec{k}^{1/2}}{r^{1/2}} \left(\frac{J_{1/2}}{kr} - J_{3/2} \right) k dk. \tag{9.9}$$

We can now transform our perturbations from k space into real space using a Hankel transform.

Unfortunately, due to the numerical restrictions discussed in the previous chapter, we do not cover a sufficient k range to apply the Hankel algorithm with enough resolution to observe interesting perturbations. The maximum resolution is proportional to $2\pi/k_{\max}$ and as we saw earlier, $k < 3\text{Mpc}^{-1}$, and as such, x can only be sampled roughly every 2 Mpc, and we wish for

perturbations that are between 10-100 kpc.

9.3 Distribution Function in Real Space

The other real space quantity of interest is the distribution function. To obtain it, we must transform $\Psi(\vec{k}, \tau, q\hat{n})$. Unlike the perturbations that we transformed earlier, Ψ is not spherically symmetric due to the presence of $P_l(\hat{k} \cdot \hat{n})$. As such, we cannot perform the Hankel transform. We will need to perform a full 3D Fourier transform. Before we attempt to numerically perform this, let us see if we may simplify the integrand.

We begin by defining the three vectors of interest, $\vec{k}, \vec{q}, \text{and} \vec{x}$. We have some freedom on how to define these vectors. Due to azimuthal symmetry, we know that our final solution must depend on only $\hat{x} \cdot \hat{n}$. As such, we can set the direction of $\hat{x}$, and place $\hat{n}$ in the same plane. The simple way of doing this is by setting $\hat{x}$ in the $\hat{z}$ direction and place $\hat{n}$ in the xz plane. We leave $\hat{k}$ as a free vector, as we will be integrating over all of k-space in our Fourier transform. The final form of our three vectors are

$$\hat{x} = \hat{z}, \tag{9.10a}$$

$$\hat{n} = \sin(\alpha)\hat{x} + \cos(\alpha)\hat{z}, \tag{9.10b}$$

$$\hat{k} = \cos(\theta)\sin(\phi)\hat{x} + \sin(\theta)\sin(\phi)\hat{y} + \cos(\phi)\hat{z}, \tag{9.10c}$$

where $\alpha = \hat{x} \cdot \hat{n}$.

We may perform the appropriate dot products and rewrite our Fourier

transform as

$$\begin{aligned}\Psi(\vec{x},\vec{q},\tau) = \int e^{-ikx\cos\phi}\sum_{l=0}^{\infty}(-i)^l(2l+1)\Psi_l(\vec{k},\vec{q},\tau)\\ P_l(\sin(\alpha)\cos(\theta)\sin(\phi)+\cos(\alpha)\cos(\phi))\\ d\phi d\theta\sin(\theta)F(k)k^2dk,\end{aligned} \tag{9.11}$$

where $F(k)$ is again the k space representation of the initial conditions.

We may now perform the angular integral analytically. We obtain

$$\begin{aligned}\Psi(\vec{x},\vec{q},\tau) = 4\pi\int\sum_{l=0}^{\infty}(2l+1)P_l(\alpha)\frac{1}{(kx)^{l+1}}\\ \left(\sum_{m=0,even}^{l}\theta_m(kx)\sin(kx)(-1)^{m/2}\right.\\ \left.+\sum_{m=1,odd}^{l}\theta_m kx\cos(kx)(-1)^{(m+1)/2}\right)F(k)k^2dk,\end{aligned} \tag{9.12}$$

where $\theta_m(x)$ are the reverse Bessel polynomials and are defined as[6]

$$\theta_n(x) = \sum_{m=0}^{n}\frac{(2n-m)!}{(n-m)!m!}\frac{x^m}{2^{n-m}}, \tag{9.13a}$$

$$\theta_n(x) = \sum_{m=0}^{n}C_{nm}\frac{x^m}{2^{n-m}}. \tag{9.13b}$$

The closed form of this expression was found by inputting the numerical results of integrating over P_l into the Online Encyclopedia of Integer Sequences [13].

Having determined an analytic equation, we must now consider how to numerically compute this integral. The analytic solution works well for

$kx > 0.3$ but begins to have numerical issues for small values of kx. By Taylor expanding the solution, we obtain

$$\Psi(\vec{x},\vec{q},\tau) \approx 2\pi \int \sum_{l=0}^{\infty} P_l(\alpha)(2l+1) \sum_{n=0}^{\infty}\left[\frac{kx^n(-1)^n}{C_{nn}} + \sum_{m=1}^{\infty}\frac{kx^{n+2m}(-1)^{n+m}}{C_{nn}\prod_{l=1}^{m} 2l(2m+1+2l)}\right] k^2F(k)dk, \tag{9.14}$$

which converges rapidly for small values of kx. We will hence use the analytic solution for $kx > 0.3$ and the Taylor expansion for $kx \leq 0.3$. We can now numerically perform the k space integral to obtain the distribution function in real space. To perform this integral, we integrate starting at a small value of k and end at a large value of k instead of integrating from 0 to ∞. This can be done since for a small k, $F(k)$ approaches 0, and the Taylor expansion portion approaches one. This gives us a k^2 dependance overall, causing small values to contribute little to the integral. As for the high k regime, we see that the highest power in k is proportional to $kF(k)(\sin(k)$ or $\cos(k))$. For a spherically symmetric top hat of radius R, $F(k) = 4\pi\frac{\sin(kR)-Rk\cos(kR)}{k^3}$. As such, for large k values, the integrand is proportional to k^{-1} or lower powers, and, we may stop at some maximum k without incurring large errors. To obtain the distribution function, we simply substitute Ψ we calculate into equation (5.3).

In order to determine that this routine is valid, one may compare the distribution functions with the perturbations. There should be a peak in the distribution function related to δ and the peak should be displaced from

$\vec{q} = 0$ by $\vec{v}$.

Chapter 10

Conclusion

With the amount of matter that is dark matter, it is important to fully understand the behaviour of dark matter in structure formation. Using the Conformal Newtonian gauge, we have obtained a system of equations to evolve a variety of particle types through time. Using such equations, we have been able to create a WDM+pf system and evolve it. Due to numerical complications we have a limited range of k values that may be calculated. Also, through the study of test cases, we have observed that some numerical issues exist in our solver. After obtaining accurate transfer functions, we would be able to transform our data into real space.

Once we have real space data, it would be possible to use it to generate initial conditions for an N-body simulation. Our current set of equations is linear, and as such, once the over density approaches 1, the equations become inaccurate. Hence, the N-body simulation is necessary to obtain the later evolution. We should note that due to the transitional properties of WDM, we must evolve it until it is non-relativistic, before inputting it into an N-body simulation. This N-body simulation would allow us to observe how the WDM collapses and give us new insight in structure formation in our Universe.

Bibliography

[1] Planck Collaboration. Planck 2013 results. XVI. cosmological parameters. Mar 2013, 1303.5076.

[2] A. Del Popolo. Non-baryonic dark matter in cosmology. 2013, 1305.0456.

[3] S. Dodelson. *Modern Cosmology*. Academic Press, San Diego: London: Burlington, first edition, 2003.

[4] Adrienne L. Erickcek and Kris Sigurdson. Reheating effects in the matter power spectrum and implications for substructure. *Phys. Rev. D*, 84:083503, Oct 2011.

[5] J. R. Gott, III and J. E. Gunn. The coma cluster as an x-ray source: Some cosmological implications. *Astrophys. J.*, 169:L13, Oct 1971.

[6] HL Krall and Orrin Frink. A new class of orthogonal polynomials: The bessel polynomials. *Transactions of the American Mathematical Society*, 65(1):100–115, 1949.

[7] Hannu Kurki-Suonio. Introduction to cosmological perturbation theory. Lecture notes, Apr 2011.

[8] Julien Lesgourgues and Thomas Tram. The cosmic linear anisotropy solving system (class) IV: efficient implementation of non-cold relics. *JCAP*, 1109:032, 2011, 1104.2935.

[9] Chung-Pei Ma and Edmund Bertschinger. Cosmological perturbation theory in the synchronous versus conformal newtonian gauge. *Astrophys. J.*, 1994, astro-ph/9401007.

[10] Shmuel Nussinov. Some aspects of new cdm models and cdm detection methods. *Mod.Phys.Lett.*, A24:2213–2223, 2009, 0907.3866.

[11] A. Papoulis. *Systems and Transforms With Applications in Optics*. McGraw-Hill series in systems science. Malabar, Florida: Robert Krieger Publishing Company, 1968.

[12] William H. Press, Saul A. Teukolsky, William T. Vetterling, and Brian P. Flannery. *Numerical Recipes in C*. Press Syndicate of the University of Cambridge, Cambridge: New York: Port Melbourne, second edition, 1988.

[13] N. J. A. Sloane. Online encyclopedia of integer sequences, Mar 2013.

[14] Shruti Thakur and Anjan A Sen. Can structure formation distinguish λ cdm from non-minimal $f(r)$ gravity? 2013, 1305.6447.

[15] David H. Weinberg, James S. Bullock, Fabio Governato, Rachel Kuzio de Naray, and Annika H. G. Peter. Cold dark matter: controversies on small scales. 2013, 1306.0913.

[16] Inc. Wolfram Research. *Mathematica*. wolfram Research, Inc, Champaign, Illinois, version 8.0 edition, 2010.